Generating Stimuli of Arbitrary Spectral Power Distributions for Vision and Imaging Research

Ivar Farup[a], Thorstein Seim[b], Jan Henrik Wold[a,b], and Jon Y. Hardeberg[a]

[a]Gjøvik University College, P.O.Box 191, N-2802 Gjøvik, Norway
[b]University of Oslo, P.O.Box 1072, Blindern, N-0316 Oslo, Norway

ABSTRACT

The spectral integrator at the University of Oslo consists of a lamp whose light is dispersed into a spectrum by means of a prism. Using a transmissive LCD panel controlled by a computer, certain fractions of the light in different parts of the spectrum is masked out. The remaining spectrum is integrated and the resulting colored light projected onto a dispersing plate. Attached to the computer is also a spectroradiometer measuring the projected light, thus making the spectral integrator a closed-loop system. One main challenge is the generation of stimuli of arbitrary spectral power distributions. We have solved this by means of a computational calibration routine: Vertical lines of pixels within the spectral window of the LCD panel are opened successively and the resulting spectral power distribution on the dispersing plate is measured. A similar procedure for the horizontal lines gives, under certain assumptions, the contribution from each opened pixel. Hereby, light of any spectral power distribution can be generated by means of a fast iterative heuristic search algorithm. The apparatus is convenient for research within the fields of color vision, color appearance modelling, multispectral color imaging, and spectral characterization of devices ranging from digital cameras to solar cell panels.

Keywords: spectral integrator, spectral power distribution, visual stimuli, color-matching experiments

1. INTRODUCTION

In modern color research, the most used equipment for generating colors is the color monitor. By means of an attached PC unit a color image of almost any spatial or temporal specification may be displayed on the monitor. The obvious shortcomings, however, are the monitor's limited color gamut and the fact that no metamers can be generated using it. These deficiencies make the color monitor an inappropriate tool within certain fields of color science, such as color-matching experiments and multispectral imaging. In these latter fields, the colorimetric characteristics of the light are, by necessity, insufficient as quality factors. What is needed for a proper treatment is spectral information, and in this respect the ideal equipment will be an instrument able of generating (within natural limits) light of any specified intensity and spectral composition. In a work by Hauta-Kasari et al.[1] a spectral synthesizer constructed to synthesize the lights corresponding to a low-dimensional color filter set is described: Collimated light incident on a concave diffraction grating is reflected and further dispersed onto a transmissive LCD panel placed in the focal plane of the concave grating. By computerized control of the LCD pixels, certain parts of apparent color spectrum is masked out, and finally the remaining transmitted light is remixed by means of a second concave grating. Although suitable for the purpose mentioned, a major drawback of a spectral synthesizer based on concave gratings is the huge intensity loss involved in such kind of dispersion. For the more general uses high intensities are needed in order to obtain small bandwidths while still staying above visual tresholds and noise.

An construction meeting these requirements is a apparatus that utilizes highly refractive prisms in place of diffraction gratings. This kind of instrument, a so-called spectral integrator, was first constructed in Basel (Switzerland) in 1968.[2–4] Four years later an upgraded version was build at the University of Oslo.[5] With this, one could in principle create a large number of spectra, but since each spectrum had to be masked out by manually cut and mounted masks, the spectra generated were in practise limited to those of optimal colors.

In order to make more complex experiments feasible, a further upgrade of the Oslo spectral integrator has recently been made.[6,7] For the masking purpose a LCD panel has been placed into the integrator, and for the control of the LCD pixels and the automation of the spectral recordings a special software has been developed.[8]

Although there are still improvements under conciderations, the aim of the present work is to give a brief decription of this new upgrade. Wheras the design of the spectral integrator is sketched in Section 2, Section 3 gives an outline of the new software (with particular focus on the calibration algoritm). Examples of potential applications of the spectral integrator are described briefly in Section 4. In the concluding Section 5 a proposal for future work is put forward.

2. THE SPECTRAL INTEGRATOR

A principal sketch of the spectral integrator is shown in Figure 1. The light source of the integrator is a high efficiency short-arc xenon lamp (2500W). This is placed in a specially designed lamphouse (L). From the house, two beams of light (solid and dashed lines) are tracked along two diagonal-symmetrical branches of an optical bench. The primary beam (solid line) is initially focused onto a water-cooled slit (S) by means of an aspherical condensor lens (C1) positioned at the beam's exit from the lamphouse. Immediately after the slit, the beam is condensed by another condensor lens (C2) and thereafter let through a collimator (Co) whose function is to make the light rays parallel. The parallel light is then dispersed through two 60 degree prisms (P1 and P2), and by means of a third condensing lens (C3), a sharp image of the slit aperture (S) is focused onto a transmissive monochrome LCD panel (LCD) lying in the focal plane of this lens. Due to the dispersion, this image forms a full color spectrum. By manipulating the pixels of the LCD panel, one can now control what fractions of the light should be let through the panel in the different parts of the spectrum. The condensing lens in front of the LCD panel has a double function in that it also images the exit aperture of the second prism (corresponding to the natural enclosure of the light beam leaving the prism) onto a dispersing plate (D) in front of the integrator. Though being, spatially, an image of the exit aperture of the second prism, the field of light focused on the dispersing plate will generally be of a color different from that of the exit aperture itself.

As an option, a biprism (B) may be inserted immediately after the second prism so that two color spectra are projected onto the LCD panel. By manipulating the LCD pixels in each region independently, two spectra of different spectral power distributions are transmitted. Thus, when the third condensor lens is positioned so that an image of the biprism is focused on the dispersing plate, what is seen is a bipartite field whose two halves, in general, are of a different color. By letting the LCD pixels be manipulated by movements of a PC-mouse, typical color-matching experiments can now be performed. By using the other branch of the optical bench (dashed line) to generate a field that surrounds the bipartite image of the biprism, it will, in this respect, also be possible to perform color-matching experiments under various adaptation conditions.

A vital part of the spectral integrator is the spectroradiometer (R) that is integrated with the optical table through an administrative PC unit (PC). Being managed by a computer, the spectroradiometer measures the various color stimuli automatically, without any manual reading or mechanical manipulation. Moreover, all measured data, including the spectral power distributions, are sorted and saved into files for further treatment/computation. As a result of the integrated design, the precision achieved both in the generation of light sources/stimuli and in the measurements of spectroradiometric data is significantly improved relative to the presision achieved by means of a manually controlled integrator (former version).

A detail of the spectral integrator in Oslo showing the mirror, LCD panel, and the dispersing plate is shown in Figure 2. The transmissive LCD panel seen uses an analog PAL video interface controlled from a Windows. In a future upgrade of the instrument, this will be replaced by a more accurate LCD panel, using digital input signals.

3. USING THE SPECTRAL INTEGRATOR FOR STIMULUS GENERATION

The spectral integrator is already a powerful instrument in itself. However, since there is no direct relation between the opened pixels of the LCD panel and the spectrum generated, and since the measurements taken by the spectroradiometer has to be recorded somehow, using it for real research is tedious. In order to cope with this, a software for controlling the spectral integrator has been developed.
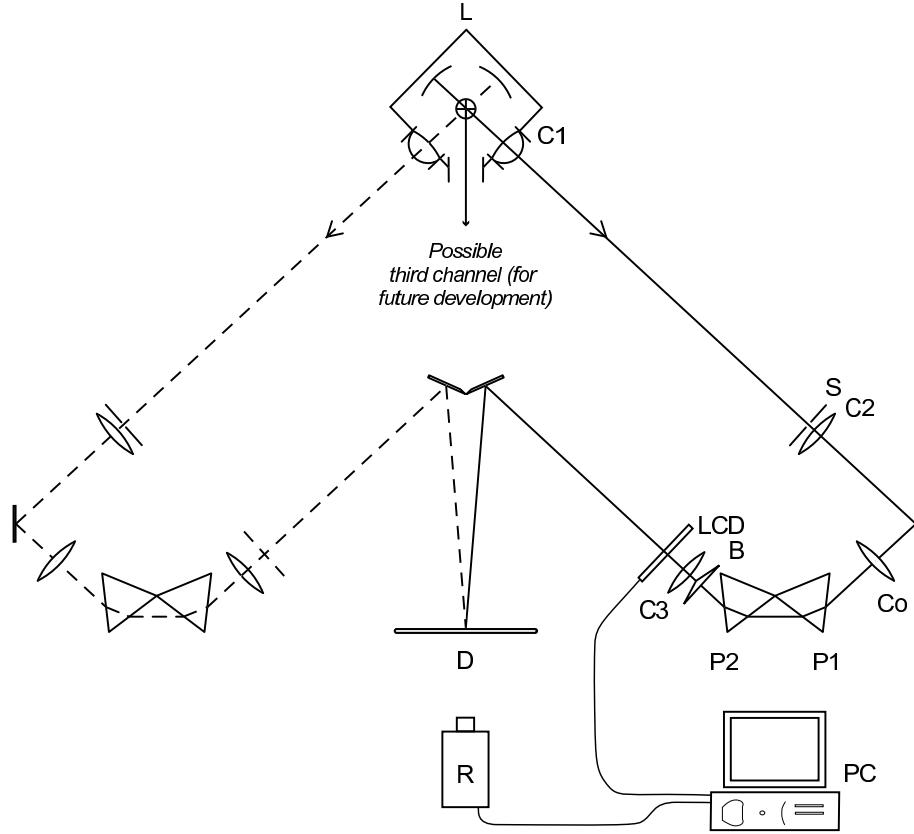
Figure 1. Principal sketch of the spectral integrator. (L) lamphouse, (C1)–(C3) condensor lenses, (S) water-cooled slit, (Co) collimator, (P1)–(P2) dispersing prisms, (LCD) transmissive LCD panel, (D) dispersing plate, (B) biprism (optional), (R) spectroradiometer, (PC) administrative PC unit.

First, a short description of the software architecture is given. Then details about characterizing and calibrating the spectral integrator are described in more detail.

3.1. Software Architecture

The executive software for the spectral integrator has been developed in Microsoft Visual Studio .NET using C++ as the development language.[8] This gives the necessary flexibility to create a graphical user interface (GUI), as well as for communicating with external devices such as the additional LCD panel and the spectroradiometer through the serial port. It also gives the necessary speed for performing the calculations needed for generating arbitrary spectral power distributions (cf. Sections 3.2–3.3).

The software is constructed as a kernel with surrounding modules. The kernel is a stand-alone Windows application, whereas the modules are implemented as DLL files which are loaded at startup. The kernel is responsible for the overall GUI as well as for facilitating communication between the modules. The modules are responsible for different subtasks, and all of the modules provide their own GUI which are included in the total GUI by the kernel.

An overall view of the software architecture is shown in Figure 3. The responsibilities of the different modules are as follows:

Spectroradiometer module: This module communicates with the spectroradiometer through the serial port. The spectroradiometer is configured, measurements requested, and results communicated.
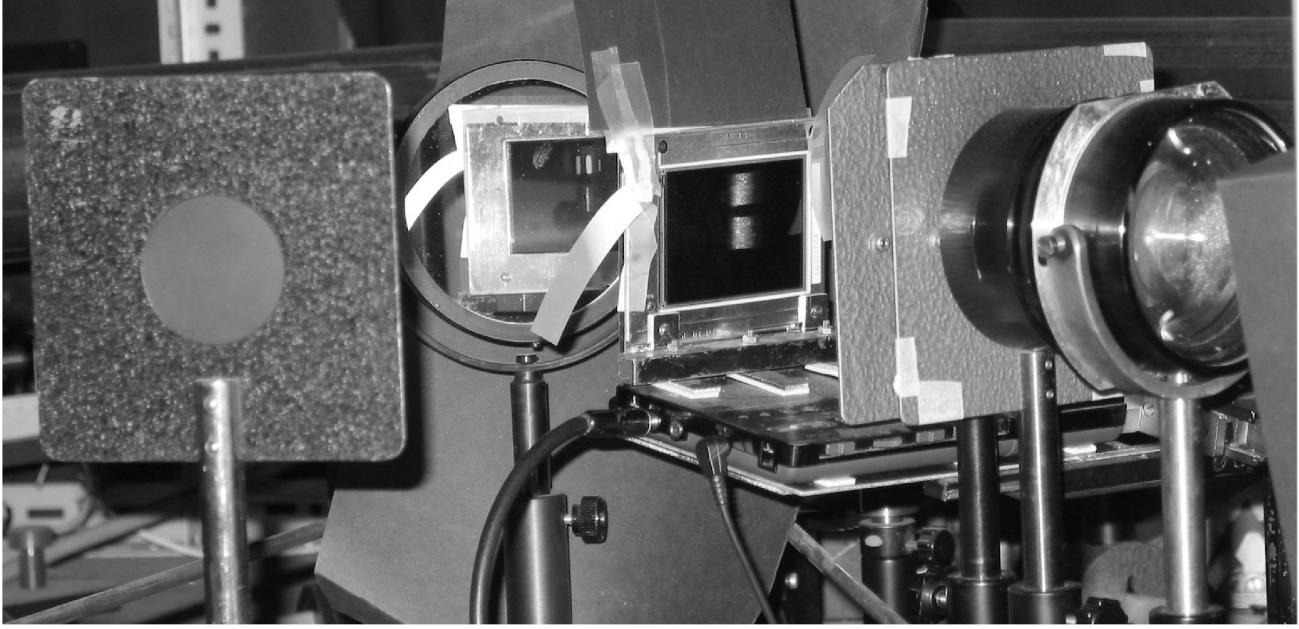
Figure 2. A detailed view of the spectral integrator prototype at UiO (from right) a lens, the transmissive LCD panel with two spectra, a mirror, and the dispersing plate onto which the resulting colored light is projected.

Calibration module: This module communicates with both the spectroradiometer module and the spectral integrator module. It asks the spectral integrator module to open certain pixels, and then asks the spectroradiometer module to measure the resulting spectrum. In this way, all data needed for the construction of the model presented in Section 3.2 are obtained.

Spectral integrator module: This module is responsible of drawing the image on the LCD panel. This can be achieved in two ways. Either, pixels can be opened individually, or a spectral power distribution can be specified. In the latter case, data from the calibration module are used in conjunction with the algorithm presented in Section 3.3.

Color matching module: This module is used for constructing color matching experiments. One reference spectral power distribution and three primary spectral power distributions can be specified. Using the input device module, the user can adjust the weights of the primaries in order to obtain color match.

Input device module: This module is in charge of communicating with the external input device used in the color matching experiments.

Primary generator module: This module is used for generating Gaussian shaped spectral power distributions.

Script parser module: When large experiments are to be performed, it is convenient to describe them through scripts. The script parser module can be used for generating such scripts utilizing the functionality supplied by all the other modules.

3.2. Characterizing the Spectral Integrator

The position of the spectrum on the LCD panel is determined by means of a binary search algorithm. First, all pixels are closed and the total energy is measured and recorded. Then, half of the panel is opened. If the energy is significantly different from the energy of the black screen, we assume that at least some part of the spectrum is inside the opened area. In this manner, we continue reducing the size of the opened part recursively until the edge of the spectrum is found. The same procedure is applied for the other three edges of the spectrum. In this way, a window N pixels wide and M pixels high is found. Typical values for the present configuration
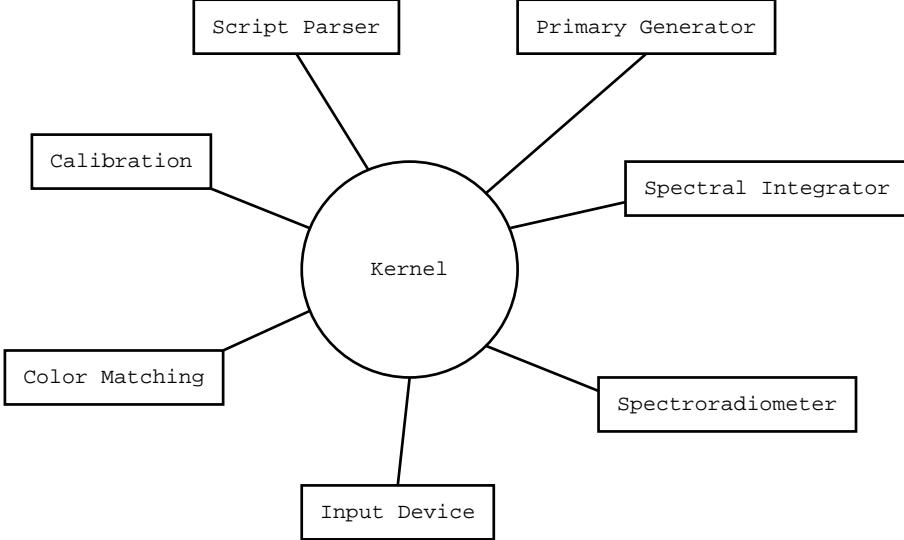
Figure 3. Overall architecture for the executive software for the spectral integrator. See Section 3.1 for details.

of the spectral integrator is $M \sim 100$ and $N \sim 200$. However, it is often convenient to combine several pixels into bigger pixel blocks consisting of, e.g., 2×2 real pixels. This is done both in order to reduce computational complexity, as well as to reduce the errors resulting from the analog PAL communication with the LCD panel. The use of blocks instead of real pixels does not affect the way we construct the algorithms below, so we will continue to refer to pixels although we might mean pixel blocks.

Spectral power distributions are in nature continuous functions of the wavelength, e.g., $s(\lambda)$. For practical purposes, the intensity of the spectral power distribution is sampled at chosen wavelengths, hence, the spectrum can be represented by a vector. In this and the following section, we will use bold face characters to denote vectors, e.g., $\mathbf{s}$.

The *black spectrum*, $\mathbf{b}$, is obtained by closing all pixels of the LCD panel, $\mathbf{b}$ being an $L \times 1$ column vector, L being the number of samples. With our spectroradiometer, the spectrum is sampled at every nanometer from 380 nm to 700 nm, hence $L = 321$. Similarly, the *white spectrum* is achieved by opening all pixels in the recently found $M \times N$ window of the LCD panel. Example black and white spectra are shown in Figure 4.

Then the so-called *aperture functions* are found by successively opening vertical lines of pixels and measuring the resulting spectral power distribution. The aperture functions are denoted $\mathbf{a}_j$, $j = 1, \ldots, N$. We remove the black spectrum to obtain

$$\overline{\mathbf{a}}_j = \mathbf{a}_j - \mathbf{b},$$
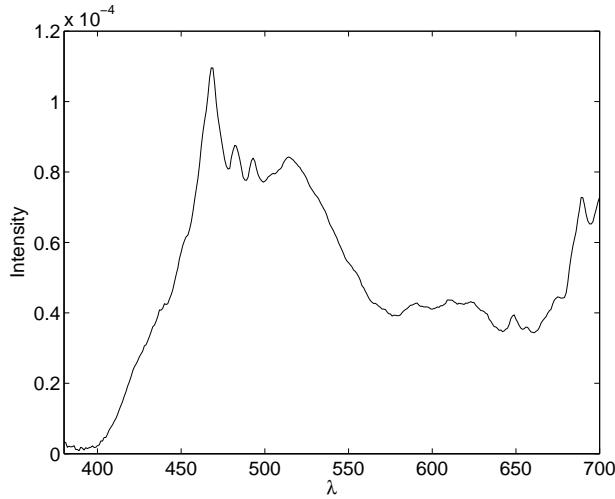
and collect the aperture functions into the $L \times N$ matrix

$$\mathbf{A} = [\overline{\mathbf{a}}_1 \ldots \overline{\mathbf{a}}_N].$$
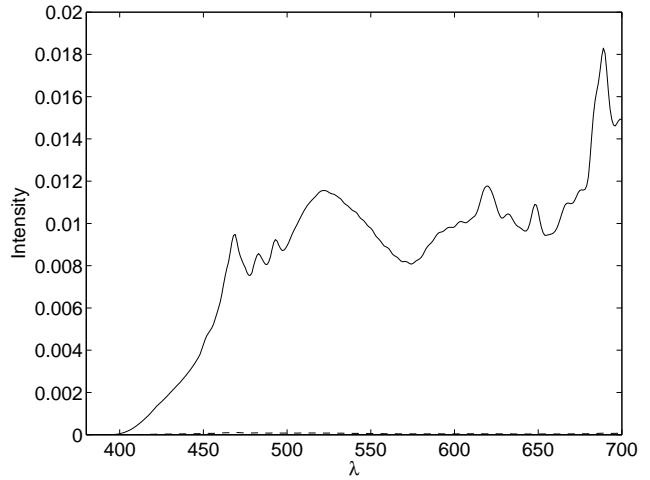
Example aperture functions are shown in Figure 4 for linewidths of two and five pixels. The plots show that the bandwidth is quite similar for two and five pixels, indicating that it is the size of the slit immediately after the light source, and not the width of the lines on the LCD panel, which gives the main contribution to the bandwidth.

Since the spectrum is not homogeneously distributed vertically over the LCD panel, a similar procedure is applied for horizontal lines. For each horizontal line opened, a spectrum similar to (but lower in intensity than) the white spectrum is achieved. These white spectra are denoted $\mathbf{v}_i$, $i = 1, \ldots, M$. Again, the black spectrum is removed:
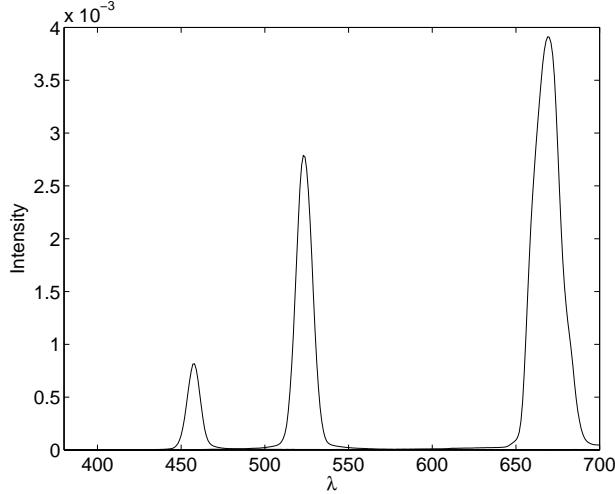
$$\overline{\mathbf{v}}_i = \mathbf{v}_i - \mathbf{b}.$$
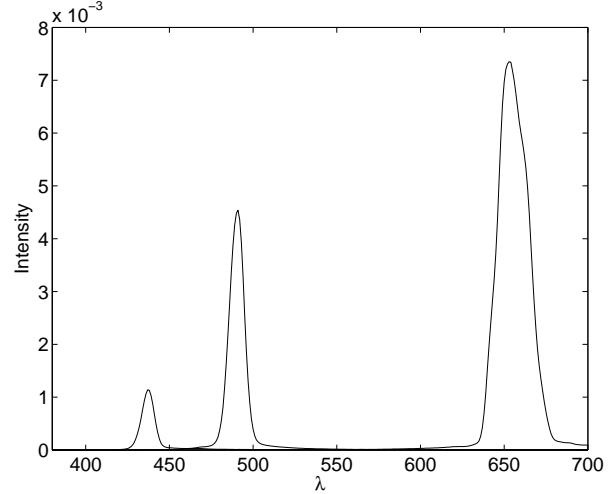
(a) Example black spectrum obtained by closing all pixels of the window on the LCD panel.

(b) Example white spectrum obtained by opening all pixels of the window on the LCD panel. The dashed line shows the black spectrum for comparison.

(c) Example aperture functions for two pixels wide vertical lines.

(d) Example aperture functions for five pixels wide vertical lines.

Figure 4. Spectral properties of the spectral integrator.

These white measurements will be used as weight factors for calculating the resulting spectrum from the aperture functions. We are, however, not interested in the weight as a function of the wavelength (index of $\overline{\mathbf{v}}_i$), but instead as a function of the pixel position. We can achieve this by locating the maxima for the aperture functions,

$$k_j = \arg\max(\overline{\mathbf{a}}_j).$$

The corresponding white measurements are then collected into a $M \times N$ weight matrix $\mathbf{W}$ whose components are given by the k_jth element of $\overline{\mathbf{v}}_i$,

$$W_{ij} = (\overline{\mathbf{v}}_i)_{k_j}.$$

Finally, the weight matrix is normalized according to

$$\overline{W}_{ij} = \frac{W_{ij}}{\sum_i W_{ij}}$$

in order to have $\sum_i \overline{W}_{ij} = 1$. $\overline{W}_{ij}$ now gives the contribution from pixel ij to the aperture function $\overline{\mathbf{a}}_j$, and the spectrum achieved by opening pixel ij is thus given as $\mathbf{s}_{ij} = \overline{W}_{ij}\overline{\mathbf{a}}_j + \mathbf{b}$ (the black noise $\mathbf{b}$ is removed from every aperture function, and added once for the resulting spectrum).

When a spectrum is to be constructed using the spectral integrator, the best control is obtained by opening neighboring pixels of the LCD panel, starting from the central horisontal line. In this way, the central part of the LCD panel – where the spectrum is most homogeneous – is used the most, and possible effects of pixel boundaries are reduced. Hence, an LCD image (a subset of all pixels) can be described by an $N \times 1$ vector $\mathbf{m}$, where $m_j \in \{0, 1, \ldots, M\}$ is the number of pixels opened at the vertical line number j starting from the central horisontal line and expanding in both directions. The weights of the various aperture functions are then given by the $N \times 1$ vector $\mathbf{w_m}$ whosecomponents are obtained by summing the weights of the opened pixels,

$$(\mathbf{w_m})_j = \sum_{i=\lfloor (M-m_j)/2 \rfloor}^{\lfloor (M-m_j)/2 \rfloor + m_j} \overline{W}_{ij}.$$

For a given LCD image described by $\mathbf{m}$, the resulting spectrum can be calculated as

$$\mathbf{s} = \mathbf{Aw_m} + \mathbf{b}. \tag{1}$$

3.3. Generation of Arbitrary Stimuli

In the previous section we deduced the forward model, i.e., the method for calculating the resulting spectral power distribution from a given image on the LCD panel as specified by the LCD vector $\mathbf{m}$. However, we are mainly interested in the reverse model, i.e., specifying a spectrum, $\mathbf{s}'$, and finding the vector $\mathbf{m}$ which results in a spectrum as close to that as possible. This can be done by, e.g., minimizing

$$||\mathbf{s}' - \mathbf{s}|| = ||\mathbf{s}' - (\mathbf{Aw_m} + \mathbf{b})||$$

with respect to $\mathbf{m}$. This is a standard non-linear constrained N-dimensional combinatorial optimization problem, and several algorithms for solving it are known.[9] However, such algorithms are generally quite time consuming and do not exploit a priori information. For color matching experiments (see Section 4.1), it is of utmost importance that spectra can be generated in real-time, giving a maximum of 40 ms (corresponding to 25 frames per second) for performing the optimization. We therefore developed the following heuristic search algorithm:

Start by setting $l = 1$ and $\mathbf{m}_l = \mathbf{0}$. The iterative algorithm then proceeds as follows:

1. Compute the spectrum $\mathbf{s}_l$ from the current estimate of $\mathbf{m}_l$ according to Equation (1).

2. Compute the difference spectrum, $\mathbf{d}_l = \mathbf{s}' - \mathbf{s}_l$.

3. For every component $(\mathbf{d}_l)_k$ of $\mathbf{d}_l$, find the aperture function $\overline{\mathbf{a}}_j$ minimizing $|k - \arg\max(\overline{\mathbf{a}}_j)|$. Construct the $N \times 1$ vector $\Delta \mathbf{m}_l$ with components given by $(\Delta \mathbf{m}_i)_j = \sum_k (\overline{\mathbf{a}}_j)_k / M$.

4. The components of $\Delta\mathbf{m}_l$ are real numbers, whereas the number of pixels to open or close must be a natural number. Experiments have shown that a simple round-off of the real numbers can lead to quite large systematic errors and cause the iterative algorithm to converge prematurely. Therefore, the rounding is performed in a manner inspired by so-called error diffusion algorithms: The first component of $\Delta\mathbf{m}_l$ is rounded towards the nearest integer, and the round-off error is added to the neighboring component. In order to further reduce systematic errors, the error diffusion is performed alternately in the two directions through the vector $\Delta\mathbf{n}_l$ depending on whether l is even or odd. The vector rounded in this manner is denoted $\Delta\overline{\mathbf{m}}_l$.

5. Update the estimate of $\mathbf{m}$ according to $\mathbf{m}_{l+1} = \min(\max(\mathbf{m}_l + \Delta\overline{\mathbf{m}}_l, 0), M)$.

6. If $\mathbf{m}_{l+1} \neq \mathbf{m}_l$, increase l and iterate from 1, else $\mathbf{m}_{l+1}$ is accepted as the best estimate for the LCD image.

The algorithm works in real-time. For simple smooth spectra, the number of iterations is typically about five, whereas for complex spectra with sharp edges, the number of iterations can approach twenty. In Figure 5, examples of spectral power distributions generated with the algorithm are shown. The plots show the specified spectrum, $\mathbf{s}'$ (shown as solid lines), the calculated closest match, $\mathbf{s}$ (shown as dashed lines) and the measured resulting spectrum, $\mathbf{m}$ (shown as dash-dot lines). The difference between the calculated closest match and the measured spectrum results mainly from the assumptions made for the forward model from Section 3.2, whereas the difference between the specified and the calculated closest match stems both from the algorithm presented above and from the physical limitations inherent to the equipment itself. For example, it is impossible to generate a higher intensity than that provided by the lamp (filtered through the optics), and this is the reason for the lack of intensity in the blue part (short wavelengths) of the spectrum. In the red part of the spectrum (long wavelengths), the unevenness in the generated spectra is considerably higher than in the other parts of the spectrum. This is related to the two facts that (1) the light source has considerably more spikes in this part of the spectrum, and that (2) the dispersion is weak in this part of the spectrum, increasing the bandwidth of the aperture functions and reducing the possibility of controlling the resulting spectral power distribution.

4. POTENTIAL APPLICATIONS

With a spectral integrator of the kind described above, the potential applications are numerous. At UiO and HiG projects of particular interest fall into the three categories of colorimetry (4.1 through 4.3), imaging (4.4 and 4.5), and light sensor characterization (4.5 and 4.6).

4.1. Transformability of Color-Matching Functions
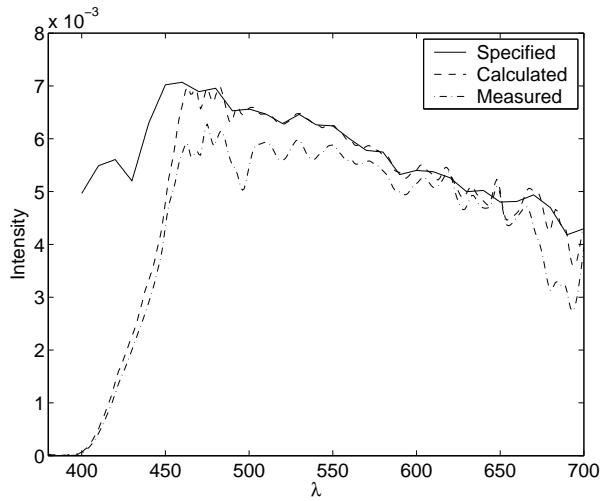
In a series of articles, W. A. Thornton[10] has questioned the assumption of linearity that found the basis of standard colorimetry. Challenged by this, the International Commission on Illumination (CIE) has established a technical committee whose mandate is to test if the transformability assumption holds true.[11] Plans have been made for a more elaborate investigation in which the transformability can be tested in detail. The spectral integrator facilitate functions which make it possible to run color-matching experiments yielding enough data for a thorough investigation.

4.2. Metamerism
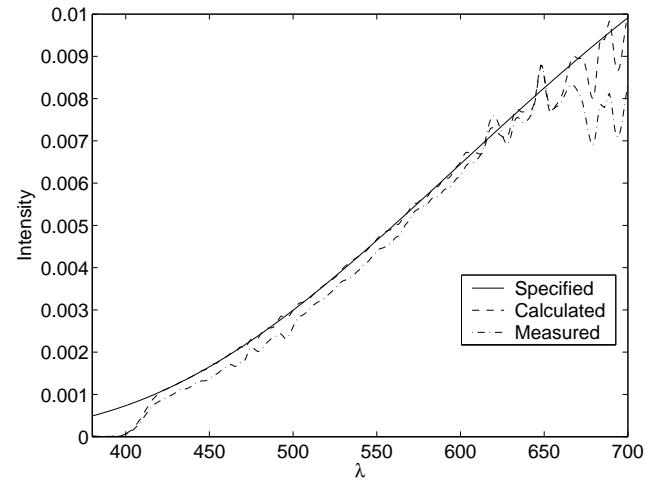
The study of metamerism is a topic in color and lighting industry. Though CRT monitors have shown powerful in color vision studies, metameric colors cannot be produced on these. The spectral integrator, however, is particularly well-suited for this kind of studies.

4.3. Chromatic Adaptation and Color Appearance Modeling
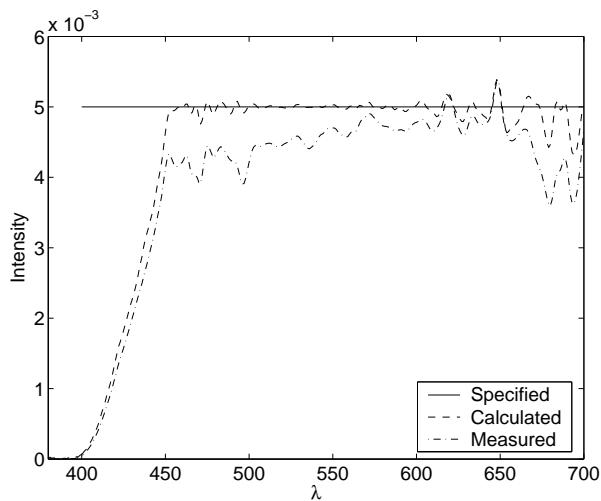
A color appearance model (CAM)[12] provides a viewing condition specific means for transforming tristimulus values to or from perceptual attribute correlates. The two major pieces of such a model are a chromatic adaptation transform[13, 14] and equations for computing correlates of perceptual attributes, such as brightness, lightness, chroma, saturation, colorfulness, and hue.[15] Color Appearance Models are capable of predicting color appearance
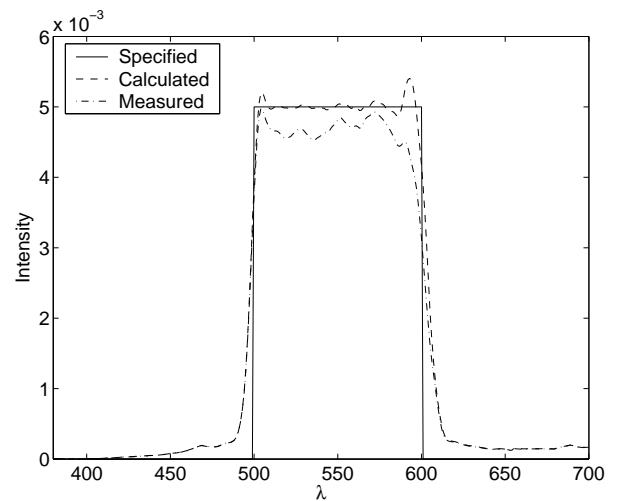
(a) CIE light source D65 as specified, calculated, and measured.

(b) CIE light source A as specified, calculated, and measured.

(c) CIE light source E as specified, calculated, and measured.

(d) Box shaped spectrum as specified, calculated, and measured.

Figure 5. Generated stimuli using the proposed heuristic search algorithm.

under a variety of viewing conditions, including different light sources, luminance levels, surrounds, and lightness of background, and are potentially a useful tool for achieving successful cross-media color reproduction.

The spectral integrator makes more detailed studies of these effects feasible. Using two LCD panels, one in each branch of the optical bench, it will be possible to specify exactly the spectral power distribution of both center and surround of a visual test field, and thus to study the effects of chromatic adaptation on both color-matching functions and color-sensation thresholds.

4.4. Multispectral Image Acquisition

For digital image acquisition and reproduction, three-channel images have several limitations, in particular because of metamerism. By augmenting the number of channels in the image acquisition and reproduction beyond three, we can remedy these problems, and thus increase the color image quality significantly. This is the basic idea of multispectral color imaging.

The most commonly used principle for acquisition of multispectral color images is to use a monochrome CCD camera coupled with an electronically tunable filter (LCTF).[16,17] However, the flexibility in choosing the spectral transmissivity of such filters leaves much to be wished for. With the spectral integrator, it is possible to completely omit the filter, and instead use the integrator as a light source with extremely flexible spectral properties. A similar technique has been used by Hauta-Kasari et al.[18] where the spectral light was produced using concave gratings, LC-panel and polarizers.

4.5. Spectral Characterization of Digital Cameras

In order to properly calibrate an electronic camera it is necessary to know the spectral sensitivity of the camera. It is possible to estimate the sensitivity indirectly by acquiring a set of samples of known spectral reflectances, and by inverting the resulting system of linear equations.[19] In the presence of noise, this system inversion is not straightforward. A more robust method consists in measuring the camera response when exposed to a set of calibrated nearly monochromatic light stimuli.[20] The spectral integrator may be an adequate device for such purposes.

4.6. Solar Cell Characterization

The ultimate method to test the overall performance of solar cells is outdoor exposure. However, reliable and reproducible results can only be obtained with solar simulators whose illumination conditions are designed to match an internationally standardized solar spectrum.

Commercially available solar simulators usually use a xenon arc lamp in conjunction with a spectral correction filter which approaches the terrestrial solar spectrum such that it is good enough for many applications.[21,22] It is possible that the spectral integrator can offer a more precise simulation of the solar spectrum, and that it therefore can be used for research and development of solar cells.

5. CONCLUSION AND FURTHER WORK

During the last decades, a spectral integrator has been built at the University of Oslo. The spectral integrator has now been extended with an executive software which through a fast iterative algorithm makes feasible the construction of arbitrary spectral power distributions with good precision. Combined with this software, the spectral integrator has applications to a wide range of fields, which will be investigated in the future.

In order to improve the properties of the spectral integrator, further investigations are planned. For generation of high precision spectra, the spectroradiometer measurements can be included in the iterative algorithm from Section 3.3 in step 1 instead of using Equation (1). This will of course make the algorithm much slower, but will be useful for generating high precision spectral stimuli. Furthermore, the behavior of the heuristic search algorithm must be tested against well established (and slower) optimization algorithms, e.g., the simulated annealing algorithm. There is a possibility that the level of precision of the algorithm itself could be improved without compromising on the real-time requirement.

REFERENCES

1. M. Hauta-Kasari, K. Miyazawa, S. Toyooka, and T. Jaaskelainen, "Spectral vision system based on rewritable broad band color filters," in *Proceedings of the International Symposium on Multispectral Imaging and Color Reproduction for Digital Archives*, pp. 155–158, (Chiba, Japan), 1999.

2. M. Gasser, H. Bilger, H.-D. Hofmann, and K. Meischer, "Spektraler Farbintegrator," *Experimentia* **XV/2**, p. 52, 1959.

3. P. Weisenhorn, "Der Spektrale Farbintegrator und seine Entwicklung," *Tagungsband Luzern* , p. 415, 1965.

4. A. Valberg, *Spektraler Farbintegrator, Kompendium*. Univ. Basel, März 1966.

5. I. Østby, "Konstruktion, Bau und Eichung eines Spektralintegrators für visuelle Farbenmessung," Master's thesis, Universitetet i Oslo (University of Oslo), 1972.

6. H. H. Razavi, "Using liquid crystal display (LCD) to modulate the visual spectrum," Master's thesis, University of Oslo, 2000.

7. T. Seim and H. Razavi, "Color generation through compete spectral control," in *Oslo International Colour Conference*, E. Wessel, ed., pp. 166–167, (Oslo, Norway), October 1998.

8. T. Søndrol, L. E. Hoel, T. Aspelund, and J. Skjerven, "Styringsprogram for spektral integrator (Executive software for spectral integrator)," hovedprosjektrapport, dataingeniørstudiet, Høgskolen i Gjøvik (Gjøvik University College), 2003.

9. C. Blum and A. Roli, "Metaheuristics in combinatorial optimization: Overview and conceptual comparison," *ACM Computing Surveys* **35**(3), pp. 268–308, 2003.

10. W. A. Thornton, "Toward a more accurate and extensible colorimetry, part 1-5," *Color Research and Application* , 1992-2000.

11. CIE, "Volunteer labs sought to test foundations of colorimetry." In the Activity Report for TC1-56 Improved Colour Matching Functions, 2001.

12. M. D. Fairchild, *Color Appearance Models*, Addison-Wesley Publishing Company, 1997.

13. J. von Kries, "Chromatic adaptation," *Festschrift der Albrecht-Ludwigs-Universität* , pp. 145–158, 1902.

14. C. Li, M. R. Luo, B. Rigg, and R. W. G. Hunt, "CMC 2000 chromatic adaptation transform: CMCCAT2000," *Color Research and Applications* **27**, pp. 49–58, 2002.

15. N. Moroney, M. D. Fairchild, R. W. G. Hunt, C. Li, M. R. Luo, and T. Newman, "The CIECAM02 color appearance model," in *Proceedings of IS&T and SID's 10th Color Imaging Conference: Color Science and Engineering: Systems, Technologies, Applications*, pp. 23–27, (Scottsdale, Arizona), 2002.

16. J. Y. Hardeberg, *Acquisition and Reproduction of Color Images: Colorimetric and Multispectral Approaches*, Dissertation.com, Parkland, Florida, USA, 2001.

17. J. Y. Hardeberg, F. Schmitt, and H. Brettel, "Multispectral color image capture using a liquid crystal tunable filter," *Optical Engineering* **41**(10), 2002.

18. M. Hauta-Kasari, K. Miyazawa, S. Toyooka, and J. Parkkinen, "Spectral vision system for measuring color images," *Journal of the Optical Society of America A* **16**(10), pp. 2352–2362, 1999.

19. J. Y. Hardeberg, H. Brettel, and F. Schmitt, "Spectral characterisation of electronic cameras," in *Electronic Imaging: Processing, Printing, and Publishing in Color*, SPIE Proceedings **3409**, pp. 100–109, May 1998.

20. H. Sugiura, T. Kuno, and H. Ikeda, "Methods of measurement for colour reproduction of digital cameras," in *Digital Solid State Cameras: Designs and Applications*, SPIE Proceedings **3302**, pp. 113–122, 1998.

21. *Solar Simulation – Solar Simulator Product Guide*, 1993. ORIEL Corporation.

22. K. Petritch, *Organic Solar Cell Architectures*. PhD thesis, Graz University of Technology, Austria, 2000.